HHS Public Access

Author manuscript

Diabetologia. Author manuscript; available in PMC 2019 June 01.

Published in final edited form as:

Diabetologia. 2018 June ; 61(6): 1435–1446. doi:10.1007/s00125-018-4579-1.

Angptl8 antisense oligonucleotide improves adipose lipid metabolism and prevents diet-induced NAFLD and hepatic insulin resistance in rodents

Daniel F. Vatner[1], **Leigh Goedeke**[1], **Joao-Paulo G. Camporez**[1], **Kun Lyu**[2], **Ali R. Nasiri**[1], **Dongyan Zhang**[3], **Sanjay Bhanot**[4], **Susan F. Murray**[4], **Christopher D. Still**[5], **Glenn S. Gerhard**[5], **Gerald I. Shulman**[1,2,3], and **Varman T. Samuel**[1,6]

[1]Department of Internal Medicine, Yale University School of Medicine, P.O. Box 208020, New Haven, CT, 06520, USA

[2]Department of Cellular & Molecular Physiology, Yale University School of Medicine, New Haven, CT, 06520, USA

[3]Howard Hughes Medical Institute, Yale University School of Medicine, New Haven, CT, 06520, USA

[4]Ionis Pharmaceuticals, Carlsbad, CA, 92008, USA

[5]Obesity Institute, Geisinger Health System, Danville, PA, 17822, USA

[6]Veterans Affairs Medical Center, 950 Campbell Ave, BLG 5 3rd floor, West Haven, CT, 06516, USA

Abstract

Aims/hypothesis—Targeting regulators of adipose tissue lipoprotein lipase could enhance adipose lipid clearance, prevent ectopic lipid accumulation and consequently ameliorate insulin resistance and type 2 diabetes. Angiopoietin-like 8 (ANGPTL8) is an insulin-regulated lipoprotein lipase inhibitor strongly expressed in murine adipose tissue. However, *Angptl8* knockout mice do not have improved insulin resistance. We hypothesised that pharmacological inhibition, using a second-generation antisense oligonucleotide (ASO) against *Angptl8* in adult high-fat-fed rodents, would prevent ectopic lipid accumulation and insulin resistance by promoting adipose lipid uptake.

Corresponding authors: Varman T. Samuel, Veterans Affairs Medical Center, 950 Campbell Ave, BLG 5 3rd floor, West Haven, CT, 06516, USA, varman.samuel@yale.edu, Daniel F. Vatner, Department of Internal Medicine, Yale University School of Medicine, P.O. Box 208020, New Haven, CT, 06520, USA, daniel.vatner@yale.edu.

Data availability Data are available on request from the authors.

Duality of interest SB and SFM report being employees and shareholders of Ionis Pharmaceuticals. The other authors declare that there is no duality of interest associated with their contribution to this manuscript.

Contribution statement DFV conceived the study, developed methodology, performed experiments, supervised the study and wrote the manuscript; LG designed and performed experiments and assisted with writing the manuscript; JGC, KL, ARN and DZ performed experiments, analysed and interpreted data; SB and SFM conceived of, designed and performed experiments in the generation of ASOs; CDS and GSG conceived, designed, and performed experiments, provided human tissues for analysis and assisted with writing the manuscript; GIS and VTS conceived the study, supervised the study and assisted with writing the manuscript. All authors revised the manuscript critically for important intellectual content, reviewed the manuscript and approved the final version. DFV and VTS are responsible for the integrity of the work as a whole.

Methods—*ANGPTL8* expression was assessed by quantitative PCR in omental adipose tissue of bariatric surgery patients. High-fat-fed Sprague Dawley rats and C57BL/6 mice were treated with ASO against *Angptl8* and insulin sensitivity was assessed by hyperinsulinaemic–euglycaemic clamps in rats and glucose tolerance tests in mice. Factors mediating lipid-induced hepatic insulin resistance were assessed, including lipid content, protein kinase Cε (PKCε) activation and insulin-stimulated Akt phosphorylation. Rat adipose lipid uptake was assessed by mixed meal tolerance tests. Murine energy balance was assessed by indirect calorimetry.

Results—Omental fat *ANGPTL8* mRNA expression is higher in obese individuals with fatty liver and insulin resistance compared with BMI-matched insulin-sensitive individuals. *Angptl8* ASO prevented hepatic steatosis, PKCε activation and hepatic insulin resistance in high-fat-fed rats. Postprandial triacylglycerol uptake in white adipose tissue was increased in *Angptl8* ASO-treated rats. *Angptl8* ASO protected high-fat-fed mice from glucose intolerance. Although there was no change in net energy balance, *Angptl8* ASO increased fat mass in high-fat-fed mice.

Conclusions/interpretation—Disinhibition of adipose tissue lipoprotein lipase is a novel therapeutic modality to enhance adipose lipid uptake and treat non-alcoholic fatty liver disease and insulin resistance. In line with this, adipose ANGPTL8 is a candidate therapeutic target for these conditions.

Keywords

Angiopoietin-like 8; Antisense oligonucleotide; Ectopic lipid; Insulin resistance; Lipoprotein lipase; NAFLD

Introduction

Ectopic accumulation of specific lipid species impairs liver and muscle insulin signalling, causes insulin resistance and accounts for the link between obesity and type 2 diabetes. However, not all obese individuals are insulin resistant. This phenotypic heterogeneity may lie in differences in adipose biology [1]. Notably, some genes linked to forms of lipodystrophy are also dysregulated in individuals with more common forms of IR [2], lending genetic support for a key role for adipose dysfunction in individuals who develop IR [3]. Thiazolidinediones (TZDs) are the only medications currently available that improve adipose function. These peroxisome proliferator activated receptor γ agonists increase adipogenesis and adipose lipid storage and decrease adipose lipolysis, effectively redistributing lipid from ectopic storage sites (liver, muscle etc.) to eutopic sites (subcutaneous adipose tissue) [4–6]. This dramatically improves insulin resistance and glycaemic control with the added benefit of reducing the risk for cerebrovascular and acute coronary events [7, 8]. TZDs are also beneficial in individuals with type 2 diabetes and non-alcoholic fatty liver disease (NAFLD) or non-alcoholic steatohepatitis [9–11]. Unfortunately, numerous side effects (e.g. weight gain, volume retention and osteoporotic fractures) limit the clinical utility of TZDs [12]. Thus, newer agents are needed.

The transfer of lipids from circulating lipoproteins to tissues is largely catalysed by lipoprotein lipase (LPL) and is tightly regulated. The combined effect of a cohort of endogenous activators and inhibitors determines the quantity, timing and location of tissue

lipid uptake during feeding and fasting [13, 14]. Changes in endogenous regulators of LPL can influence the propensity for insulin resistance. For example, alterations in the LPL inhibitor APOC3 have been seen in individuals with an increased susceptibility to insulin resistance [15, 16]. Thus, pharmacological modulation of endogenous LPL regulatory factors to promote the storage of lipid in eutopic sites may be a novel paradigm to prevent or treat insulin resistance and NAFLD.

The angiopoietin-like (ANGPTL) proteins ANGPTL3, ANGPTL4 and ANGPTL8 are a family of differentially-regulated LPL inhibitors [14]. ANGPTL8 was once thought to have a trophic effect on pancreatic beta cells, although this is no longer believed to be the case [17–19]. Circulating ANGPTL8 is lower in humans with dyslipidaemia (with the caveat that circulating ANGPTL8 in humans has never been measured with a validated assay), particularly those with low HDL-C or high triacylglycerols [20]. However, ANGPTL8's primary functions may be better ascribed to local, tissue-specific actions. ANGPTL8 is an LPL inhibitor that is expressed strongly in the white adipose tissue (WAT) [17, 21]; it complexes with circulating ANGPTL3 to potently inhibit LPL [22]. Notably, ANGPTL8 expression is increased by insulin stimulation [23], so in the immediate postprandial period, a high level of circulating insulin increases ANGPTL8 expression and decreases adipose tissue LPL action and lipid uptake, potentially balancing insulin's primary actions at adipose tissue, suppression of lipolysis and promotion of lipid storage.

Surprisingly, *Angptl8* knockout mice do not manifest a dramatic metabolic phenotype [24], exhibiting no change in glucose tolerance or insulin tolerance and no meaningful effect on ectopic tissue triacylglycerol content. Nonetheless, pharmacological knockdown of ANGPTL8 expression may provide new insights into the relationship between endogenous regulation of LPL activity and the deposition of ectopic lipid and lipotoxic insulin resistance. In this study, we used a second-generation 2′-*O*-methoxy ethyl antisense oligonucleotide (ASO) against ANGPTL8 in rats and mice, evaluating the potential for adipose-specific disinhibition of LPL to prevent ectopic lipid deposition and lipid-induced insulin resistance.

Methods

Animals

Male Sprague Dawley (SD) rats (250–275g) and C57BL/6 mice (8–11 weeks old) were obtained from Charles River Laboratories (Waltham MA, USA) and Jackson Laboratory (Bar Harbor ME, USA), respectively. Animals were housed under controlled temperature (23°C) and lighting (12 h light/dark cycle, lights on at 07:00) with free access to water and food. For the hyperinsulinaemic–euglycaemic clamp study, jugular venous and carotid artery catheters were placed; for the mixed-meal tolerance tests (MMTTs), jugular venous and gastric catheters were placed. Rodents were maintained on standard regular chow (RC) (Envigo 2108S, Envigo, Madison WI, USA); or rats were placed on a high-fat diet (HFD; Research Diets D12451, Research Diets, New Brunswick NJ, USA); or mice were placed on an HFD (Research Diets D12492). Rodents were treated with 2′-*O*-methoxyethyl chimeric ASO against *Angptl8* or with a control ASO that does not target any known rat, mouse or human gene; ASO was delivered intraperitoneally (25 mg kg^{-1} $week^{-1}$). Basal tissues were taken after a 6 h fast and infusions were performed after a 12–16 h fast.

All procedures were approved by the Institutional Animal Care and Use Committee of the Yale University School of Medicine. Surgeries were performed under isoflurane anaesthesia and carprofen analgesia was provided in the postoperative period. Animals were killed either with intravenous pentobarbital or under isoflurane anaesthesia. Care was taken throughout the study to minimise suffering.

Tissue lipid isolation and measurements

All lipids were extracted from tissues in 2:1 chloroform:methanol. For hepatic diacylglycerol measurements, lipids were first extracted from cytosolic/lipid droplet and membrane-associated fractions by a modification of a previously published protocol [25]. Homogenates were separated by ultracentrifugation. The pellet contains plasma membrane lipids while the supernatant contains cytosolic lipids, including lipid droplets. The chloroform:methanol extraction was then performed from each fraction. Lipids from the organic layer were resuspended in hexane:methylene chloride:ether (89:10:1). Diacylglycerols were separated from triacylglycerols using a diol-bonded solid-phase extraction column (Waters, Milford MA, USA) [26]. Triacylglycerols were measured using the Triglyceride-SL kit (Sekisui, Charlottetown PEI, Canada). Diacylglycerols and ceramides were measured by LC-MS/MS [26].

Plasma biochemical analysis

Glucose concentrations were determined using a YSI 2700 select (Yellow Springs Instruments, Yellow Springs OH, USA) or a standard kit (Sekisui). Kits were also used to measure NEFAs (Wako, Mountain View CA, USA) and triacylglycerols (Sekisui). Insulin was measured by radioimmunoassay (EMD Millipore, Burlington MA, USA). Leptin was measured by ELISA (Abcam, Cambridge, UK).

Hyperinsulinaemic–euglycaemic clamp studies

Clamps were performed as previously described [27, 28] with primed-continuous infusion of [6,6-$^{2}H_2$]glucose tracer with a 2 h basal period and a 2 h period in which the rats received insulin (4 mU kg^{-1} min^{-1}). During the clamp period, the 20% dextrose solution used to maintain euglycaemia was enriched with tracer to approximately 2.5%.

Lipoprotein lipase activity assay

Plasma LPL activity was assessed by a fluorometric assay (Cell Biolabs, San Diego CA, USA). Adipose tissue LPL activity was determined by incubation of 80–120 mg adipose tissue at 37°C for 1 h in PBS (Sigma, St. Louis MO, USA) with 5 U/ml heparin (Sagent, Schaumburg IL, USA) and 2 mg/ml bovine serum albumin (Sigma); samples were centrifuged (900 *g*, 4°C, 15 min) and supernatant LPL activity assayed in the presence of heat-inactivated rat serum with a fluorometric kit (Cell Biolabs).

MMTTs

A mixed meal (1.16 ml/kg vegetable oil labelled with 1.8 MBq/ml ^{3}H triolein [Perkin Elmer, Waltham MA, USA] or 0.21 MBq/ml ^{3}H retinyl palmitate [American Radiolabeled Chemicals, St. Louis MO, USA] and 2.84 ml/kg Ensure Plus [Abbott Nutrition, Columbus

OH, USA]) was delivered through gastric catheters, while blood was collected from venous catheters.

Tissue solubilisation for scintillation counting

Tissues were solubilised (in 400 mM sodium hydroxide, 1% NP-40, 1% Triton X-100). Liver samples were decolourised in 1.5% hydrogen peroxide at 50°C. Samples were mixed with scintillation cocktail (Ultima Gold, Perkin Elmer) and beta counting was performed.

IPGTT

IPGTTs were conducted as previously described [29]. Mice were injected intraperitoneally with glucose (1 mg/kg body weight). Blood samples were taken by tail bleed.

Body composition and metabolic cage studies

Murine body composition was measured by ^{1}H magnetic resonance spectroscopy (Bruker, Billerica MA, USA). Energy expenditure and caloric intake were measured in a Comprehensive Laboratory Animal Monitoring System (CLAMS; Columbus Instruments, Columbus OH, USA).

Western blotting

Proteins from tissue lysate were resolved by SDS-PAGE using a 4–12% gradient gel and electroblotted onto polyvinylidene difluoride membranes (EMD Millipore). Secondary antibodies were horseradish peroxidase-conjugated (Cell Signaling Technology, Danvers MA, USA) and detection was performed with enhanced chemiluminescence. For protein kinase Cε (PKCε) translocation, cytoplasm and plasma membrane fractions were separated by ultracentrifugation as previously described [30, 31]. Proteins assessed are listed in Table 1 and ESM Table 1.

Quantitative PCR

RNA was extracted with a standard kit (RNeasy, Qiagen, Germantown MD, USA). cDNA was generated with the QuantiTect Reverse Transcription Kit (Qiagen). Abundance of transcripts was assessed by real-time PCR with a SYBR Green detection system (Bio-Rad, Hercules CA, USA). Expression for the genes of interest and an invariant control were determined using amplification efficiencies [32]. Genes assessed are listed in Table 1 and ESM Table 2.

PKCε activity assay

The PKCε activity assay is modified from previously described assays [33, 34] with reagents from a commercially available PKC assay kit (EMD Millipore). Liver tissue was homogenised and protein was extracted; 500 μg of hepatic protein was diluted in immunoprecipitation (IP) buffer and precleared with protein A/G agarose beads. IP was performed with anti-PKCε antibody (Cell Signaling). IP beads were washed and resuspended in PKC reaction buffer. The PKC activity kit was used to assess PKC activity, with 0.37 MBq [γ-^{32}P] ATP per reaction for detection.

Human adipose and liver tissue

Visceral WAT and liver biopsies were obtained intra-operatively from individuals with extreme obesity undergoing bariatric surgery at the Geisinger Clinic (Danville PA, USA). Liver tissue was preserved in formalin for histological analysis [35]. Adipose tissue was preserved in RNALater (Qiagen) and stored at −80°C [36]. Individuals were enrolled in a standardised clinical programme at the Center for Nutrition and Weight Management during which phenotypic data were collected as previously described [37]. All research participants provided written informed consent using protocols adherent to the Code of Ethics of the World Medical Association (Declaration of Helsinki). The Institutional Review Boards of Geisinger Health System and the Temple University School of Medicine approved the research.

Statistical analysis

Statistical analysis was performed using GraphPad Prism 7 (GraphPad Software, La Jolla CA, USA). Groups were compared by the Student's unpaired *t* test or a one-way ANOVA analysis followed by Tukey's Multiple Comparison test. One-way ANCOVA analysis was performed using a web-based calculator provided by Vassar College (vassarstats.net; 14/12/2017). All data are expressed as mean ± SEM. *p* values less than 0.05 were considered significant.

Results

Adipose ANGPTL8 expression is increased in insulin-resistant adults

Visceral adipose tissue biopsies were obtained from a cohort of BMI-matched obese individuals categorised as 'insulin sensitive' (HOMA-IR < 3) or 'insulin resistant' (HOMA-IR > 7) (Table 2). Diabetic individuals taking a TZD were excluded. As expected, individuals with insulin resistance had lower plasma HDL-C and higher plasma triacylglycerol concentrations. Insulin-resistant individuals also had more advanced NAFLD, as reflected by higher NAFLD activity scores on liver biopsy (Table 2). *ANGPTL8* gene expression normalised to TATA-binding protein gene expression was 7.6-fold higher ($p < 0.05$) in insulin-resistant individuals as compared with the insulin-sensitive individuals (Table 2).

Increased adipose ANGPTL8 expression could reduce postprandial adipose LPL activity and predispose to NAFLD. We performed a series of rodent experiments to determine if inhibiting ANGPTL8 with a specific ASO prevented ectopic lipid accumulation and insulin resistance.

Angptl8 ASO treatment reduces fasting plasma triacylglycerols and insulin in fat-fed rats

Three weeks of *Angptl8* ASO treatment in HFD-fed male SD rats decreased fasting *Angptl8* expression by 73% in the epididymal fat pad and 82% in the liver. The expression of other hepatic negative regulators of LPL such as *Angptl3*, *Apoc3*, and *Apoe* was increased (ESM Fig. 1a,b). ASO treatment did not cause transaminitis or changes in plasma blood urea nitrogen (BUN). Body weight was not different, though it did tend to be lower (ESM Fig. 1c, Table 3). As expected, *Angptl8* ASO decreased fasting plasma triacylglycerol (59%

reduction; Table 3). Plasma glucose after a 6 h fast was unchanged, while plasma insulin was reduced by 54% (Table 3), consistent with improved insulin sensitivity. There was no difference in leptin and adiponectin levels after an overnight fast (ESM Table 3). Macrophage-associated gene *Cd68* expression was modestly increased in overnight fasted adipose tissue (ESM Table 3).

Angptl8 ASO treatment prevents lipid-induced hepatic insulin resistance

HFD-fed male SD rats were treated with ASO for 3 weeks; whole-body and tissue-specific insulin action was assessed by the hyperinsulinaemic–euglycaemic clamp technique in awake, unrestrained animals. *Angptl8* ASO-treated rats had a slightly lower body weight prior to clamp (control ASO: 424 g ± 13; *Angptl8* ASO: 382 g ± 7; $p < 0.01$), potentially due to slower recovery from surgery. The glucose infusion rate required to maintain euglycaemia was similar between the two groups (Fig. 1a–b) and insulin-stimulated whole-body glucose disposal was also unchanged (Fig. 1c). Basal rates of endogenous glucose production, reflecting hepatic glucose production, were unchanged between control and *Angptl8* ASO-treated groups (Fig. 1d). *Angptl8* ASO had no impact on insulin-stimulated whole-body glucose disposal (Fig. 1c) but improved the suppression of endogenous glucose production (Fig. 1d–e). Surprisingly, plasma insulin concentration was approximately 17% lower during the clamped portion of the experiment ($p < 0.05$). Insulin-mediated suppression of circulating NEFA concentration was not changed by *Angptl8* ASO treatment (Fig. 1f). Thus, *Angptl8* ASO specifically improved hepatic insulin sensitivity.

Angptl8 ASO attenuates HFD-induced hepatic steatosis

Angptl8 ASO reduced hepatic triacylglycerol content by 66% in comparison with control ASO-treated rats (Fig. 2a). Total diacylglycerol content was reduced in *Angptl8* ASO-treated rats (Fig. 2b). Diacylglycerol (DAG) was reduced both in a plasma membrane fraction and in a lipid-droplet-containing cytoplasmic fraction (did tend to be lower (ESM Fig. 2). The primary DAG species in both control and *Angptl8* ASO-treated groups contained C18:1, C18:2 and C16:0 fatty acyl moieties, largely reflecting the lipid content of the lard-based diet. Total hepatic ceramide content was unchanged (Fig. 2c). Two ceramide species implicated in resistance, C16 ceramides [38, 39] and C18 ceramides [40], were actually increased. C24:1 ceramides were elevated, while C20 ceramides were decreased (did tend to be lower (ESM Fig. 3).

DAGs impair hepatic insulin signalling by activating PKCε, which phosphorylates the insulin receptor at an inhibitory threonine, thereby reducing insulin receptor signalling through Akt [41, 42]. Hepatic PKCε enzymatic activity was decreased by 43% in Angptl8 ASO-treated rats (Fig. 2d). Similarly, PKCε translocation to the plasma membrane, a readout of novel PKC activation, was decreased by 51% in Angptl8 ASO-treated rats (Fig. 2e). Improved hepatocellular insulin action was reflected in improved insulin stimulation of hepatic Akt phosphorylation (Fig. 2f).

Angptl8 ASO treatment increases adipose tissue chylomicron triacylglycerol uptake

We hypothesised that *Angptl8* ASO prevents ectopic lipid accumulation by enhancing adipose lipid uptake. *Angptl8* ASO did not affect plasma or epididymal adipose LPL activity

(Figs 3a,b). However, subcutaneous adipose LPL activity was increased by approximately threefold (Fig. 3c). We quantified adipose tissue mealtime triacylglycerol clearance with labelled MMTTs. Mixed meals were given in combination either with ^{3}H-retinyl palmitate or, in a separate cohort, ^{3}H-triolein. Retinyl palmitate is primarily taken up by the liver and is used to quantify hepatic chylomicron remnant clearance. Triolein is used to quantify fatty acid uptake into all lipid-storing tissues. To avoid possible effects of altered body weight on triacylglycerol clearance, these studies were performed after one week of treatment with ASO when *Angptl8* gene expression was decreased by half (did tend to be lower (ESM Fig. 4a) without body weight divergence; ASO was given during the last week of the 4 week fat-feeding period.

Hepatic retinyl palmitate uptake 4 h after delivery of the mixed meal was similar between control ASO and *Angptl8* ASO-treated rats (Fig. 3e), suggesting that chylomicron remnant clearance was unchanged by *Angptl8* ASO. MMTTs with triolein label were performed in both insulin-sensitive RC-fed rats and in insulin-resistant 4 week HFD-fed rats (Fig. 3 and ESM Fig. 5). The ratio of adipose triolein uptake per gram of adipose to hepatic triolein uptake per gram of liver was measured. Under both RC- and HFD-fed conditions, plasma triacylglycerol concentrations were reduced during the MMTT in *Angptl8* ASO-treated rats (Fig. 3d and ESM Fig. 5a). Subcutaneous adipose triacylglycerol uptake was increased in the RC-fed *Angptl8* ASO-treated rats (ESM Figs 5b,c). In HFD-fed rats, incorporation of labelled triolein was increased by *Angptl8* ASO in both subcutaneous and epididymal adipose tissue (Figs 3f,g). Together, these data demonstrate that reducing *Angptl8* expression enhances adipose lipid uptake.

Angptl8 ASO protects fat-fed mice from hepatic steatosis and insulin resistance

We assessed the robustness of the effect of *Angptl8* ASO in a second rodent model, the HFD-fed C57BL/6 mouse, a widely studied preclinical model of diet-induced insulin resistance that also enables us to perform indirect calorimetry to assess energy balance.

Three weeks of *Angptl8* ASO treatment reduced fasting ANGPTL8 expression by 43% (ESM Fig. 4b), and fat-fed *Angptl8* ASO-treated mice had 37% less hepatic triacylglycerol than control ASO-treated mice (Fig. 4a). Furthermore, IPGTTs were performed. Plasma glucose after intraperitoneal glucose injection was unchanged by *Angptl8* ASO but the insulin level required to maintain these glucose levels was significantly reduced (Figs 4b,c).

Angptl8 ASO alters body composition but not net energy metabolism in mice

We assessed the effect of ANGPTL8 knockdown on calorie intake and energy expenditure. Metabolic cage experiments were performed with both RC-fed and HFD-fed cohorts of C57BL/6 mice. *Angptl8* ASO did not alter the growth curve of mice on either diet (Figs 5a,b). *Angptl8* ASO treatment decreased body-fat percentage in RC-fed mice (Fig. 5c) but increased body-fat percentage in HFD-fed mice (Fig. 5d). *Angptl8* ASO had no measurable effect on food intake in RC-fed mice, but reduced food intake in HFD-fed mice (Figs 5e,f). As assessed by ANCOVA, energy expenditure correlated with muscle mass in both RC-fed mice (R^2=0.51) and HFD-fed mice (R^2=0.62); adjusted for muscle mass, *Angptl8* ASO had

no effect on energy expenditure in RC-fed mice (p=1.0) while it reduced muscle-mass-adjusted energy expenditure in HFD-fed mice (p<0.001) (Figs 5g,h and ESM Fig. 6).

Discussion

Adipose dysfunction leads to ectopic lipid deposition and, in turn, insulin resistance, type 2 diabetes, NAFLD and cardiovascular disease. Improving adipocyte function with TZDs is a well-established treatment for all these conditions [4, 7–9, 11]. However, weight gain, fluid retention and increased fracture risk limit their clinical utility. Adipose lipid storage could be improved by enhancing adipose LPL activity, potentially through targeting ANGPTL8. This paradigm would leverage a specific biological effect to achieve the same clinical benefits as TZDs, while minimising off-target adverse effects. However, *Angptl8* knockout mice did not demonstrate significant improvements in ectopic lipid or glucose metabolism [24]. In contrast, the data in this study suggest that dysregulation of ANGPTL8 is associated with NAFLD and insulin resistance, and pharmacological inhibition using a second-generation ASO against *Angptl8* improves adipose function, increasing postprandial triacylglycerol uptake and preventing ectopic lipid accumulation and lipid-induced insulin resistance.

We observed an association between adipose *ANGPTL8* expression and metabolic disease. Prior studies of ANGPTL8 in human blood reported increases in circulating protein in individuals with the metabolic syndrome [43] and type 2 diabetes [44, 45]; furthermore, serum ANGPTL8 levels correlate with BMI [45] and hepatic steatosis [46]. However, circulating ANGPTL8 may not accurately reflect adipose tissue ANGPTL8 content and has not been measured using validated assays. We observed that in BMI-matched adult human participants with extreme obesity, increased visceral adipose ANGPTL8 expression is associated with insulin resistance and NAFLD, independent of the documented association with BMI. Increased adipose ANGPTL8 may decrease adipose LPL activity, inhibiting eutopic adipose lipid storage and promoting ectopic lipid accumulation. Adipose ANGPTL8 expression may be induced by the resulting hyperinsulinaemia, contributing to a pathogenic cycle that further sustains ectopic lipid accumulation and insulin resistance.

Our data support the hypothesis that inhibition of ANGPTL8 expression reduces ectopic lipid accumulation by improving adipose lipid uptake. First, *Angptl8* ASO increased subcutaneous adipose LPL activity and improved adipose meal triacylglycerol uptake in both RC-fed and HFD-fed rats. *Angptl8* ASO also decreased hepatic *Angptl8* expression and since the liver is a major site for ANGPTL8 expression, this could have impacted circulating ANGPTL8 and possibly plasma LPL activity [47]. However, we did not detect any change in plasma LPL activity, suggesting the physiological effect of the ASO is specifically due to its impact on adipose *Angptl8*. The lack of effect on global circulating LPL activity may in part be explained by the dramatic upregulation of other hepatically produced LPL inhibitory factors seen in the *Angptl8* ASO-treated animals.

Second, in HFD-fed rats, improved adipose lipid clearance resulted in a reduction in hepatic steatosis and an improvement in hepatic insulin action. The reduction in hepatic diacylglycerol content decreased PKCε activation and improved insulin signalling. *Angptl8* ASO-treated C57BL/6 mice were also protected from fat-feeding-induced hepatic steatosis

and had improved glucose tolerance. Notably, liver ceramide content did not correlate with changes in tissue insulin action. Taken together, these findings suggest that diversion of lipid from the liver to the adipose tissue protects rodents from hepatic DAG–PKCε mediated insulin resistance.

Some subtleties of the methodology warrant discussion. Tissue-specific triacylglycerol clearance is usually assessed by oral challenge with a labelled lipid mixture (e.g. vegetable oil with radiolabelled triolein) or intravenous challenge with radiolabelled lipoproteins. Here, we labelled the triacylglycerol component of an MMTT. This allowed us to assess the disposition of mealtime triacylglycerol from physiologically produced chylomicrons in the context of dietary carbohydrate and prandial insulin secretion. This is relevant to studies of the function of ANGPTL8, as *Angptl8* gene expression is stimulated by insulin [23]. This test may help to explain the difference between this study and the previous study of knockout mice, in which no change in adipose tissue lipid uptake was observed. Of course, there is also a difference in biology between the models, reflecting the difference between knockdown and complete knockout of ANGPTL8 (which may impact development and/or lead to compensatory changes).

The protective effects of *Angptl8* ASO are independent of changes in net energy balance or weight gain. *Angptl8* ASO did not change energy expenditure or food intake under RC-fed conditions. In HFD-fed mice, there were subtle but matched decreases in both energy expenditure and food intake. These results contrast with a recent report that a monoclonal anti-ANGPTL8 antibody increased energy expenditure and weight loss [48], a difference which may be due to the different treatment modalities. The effects of *Angptl8* ASO on body composition are intriguing. *Angptl8* ASO treatment decreased fat mass in RC-fed mice but increased fat mass accretion in HFD-fed mice. This divergence reflects the different pathways by which adipose fat is delivered with high-carbohydrate diets and HFDs. In the HFD-fed rodents, dietary fat is the main source of adipose lipid, and *Angptl8* ASO increased lipid uptake from chylomicrons into adipose tissue in HFD-fed rats. Subcutaneous adipose lipid uptake was also increased in RC-fed rats, but RC-fed mice had a decrease in overall adiposity. In RC-fed rodents, most tissue lipid is produced via hepatic de novo lipogenesis, which would be delivered to the adipose tissue in triacylglycerol-rich VLDL particles. VLDL secretion is highest in the post-absorptive state, when *Angptl8* expression is normally low, hence when *Angptl8* ASO is unlikely to increase lipid uptake. This is consistent with the prior report demonstrating decreased WAT triacylglycerol uptake of intravenously infused VLDL in *Angptl8* knockout mice [24].

These studies have some limitations. In the clamp study, the *Angptl8* ASO-treated rats were 10% smaller than control ASO-treated rats. The reduced body weight may favour improved insulin sensitivity. However, there were still improvements in glucose tolerance in the weight-matched mice and improvements in insulin level in 6 h fasted rats, suggesting that the improvements in insulin action are independent of changes in body weight. Moreover, the plasma insulin concentrations achieved during the hyperinsulinaemic–euglycaemic clamps in *Angptl8* ASO-treated rats were lower than the concentrations in the control ASO-treated rats, possibly due to increased insulin clearance. This unintended difference would reduce the observed effect of the *Angptl8* ASO on insulin resistance; under matched insulin

concentrations, an even greater suppression of hepatic glucose production in the *Angptl8* ASO-treated animals is expected.

In contrast to prior studies with adipose-specific *Angptl8* knockout mice [24], the present set of studies suggest that targeting adipose ANGPTL8 can prevent lipid-induced insulin resistance. Reduction in *Angptl8* improved adipose lipid uptake and reduced the accumulation of ectopic lipid, addressing a root cause of insulin resistance. These results are intriguing and support further study of this system, its role in modulating LPL in fed and fasted conditions, its role in modulating fat mass and possibly energy metabolism. Moreover, additional studies are needed to determine whether the increases in adipose ANGPTL8 in humans are a cause or consequence of insulin resistance. More broadly, campaigns focused on compounds that specifically activate or disinhibit adipose LPL may lead to exciting new therapeutic opportunities.

Supplementary Material

Refer to Web version on PubMed Central for supplementary material.

Acknowledgments

We would like to thank M. Kahn for LC-MS measurements; and J. Dong, G. Butrico, C. Todeasa, M. Batsu and the Yale Diabetes Research Core facility for excellent technical support. All are at Yale University School of Medicine, New Haven, CT, USA.

Funding We would like to thank our funding sources: the National Institutes of Health (K23 DK-10287, R01 DK-40936, U24 DK-059635, P30 DK-045735) and the Veterans Health Administration (Merit Review Award I01 BX000901).

Abbreviations

ANGPTL3/4/8	Angiopoietin-like 3/4/8
ASO	Antisense oligonucleotide
BUN	Blood urea nitrogen
DAG	Diacylglycerol
GINF	Glucose infusion rate
HFD	High-fat diet
IP	Immunoprecipitation
LPL	Lipoprotein lipase
MMTT	Mixed-meal tolerance test
NAFLD	Non-alcoholic fatty liver disease
PKCε	Protein kinase Cε
qPCR	Quantitative PCR

RC	Regular chow
SD	Sprague Dawley
TZD	Thiazolidinedione
WAT	White adipose tissue

References

1. Cuthbertson DJ, Steele T, Wilding JP, et al. What have human experimental overfeeding studies taught us about adipose tissue expansion and susceptibility to obesity and metabolic complications? Int J Obes (Lond). 2017; 41:853–865. [PubMed: 28077863]
2. Lotta LA, Gulati P, Day FR, et al. Integrative genomic analysis implicates limited peripheral adipose storage capacity in the pathogenesis of human insulin resistance. Nat Genet. 2017; 49:17–26. [PubMed: 27841877]
3. Shulman GI. Cellular mechanisms of insulin resistance. The Journal of clinical investigation. 2000; 106:171–176. [PubMed: 10903330]
4. Soccio RE, Chen ER, Lazar MA. Thiazolidinediones and the promise of insulin sensitization in type 2 diabetes. Cell metabolism. 2014; 20:573–591. [PubMed: 25242225]
5. Mayerson AB, Hundal RS, Dufour S, et al. The effects of rosiglitazone on insulin sensitivity, lipolysis, and hepatic and skeletal muscle triglyceride content in patients with type 2 diabetes. Diabetes. 2002; 51:797–802. [PubMed: 11872682]
6. Kim JK, Fillmore JJ, Gavrilova O, et al. Differential effects of rosiglitazone on skeletal muscle and liver insulin resistance in A-ZIP/F-1 fatless mice. Diabetes. 2003; 52:1311–1318. [PubMed: 12765938]
7. Young LH, Viscoli CM, Curtis JP, et al. Cardiac Outcomes After Ischemic Stroke or TIA: Effects of Pioglitazone in Patients with Insulin Resistance Without Diabetes. Circulation. 2017; 20:1882–1893.
8. Kernan WN, Viscoli CM, Furie KL, et al. Pioglitazone after Ischemic Stroke or Transient Ischemic Attack. The New England journal of medicine. 2016; 374:1321–1331. [PubMed: 26886418]
9. Belfort R, Harrison SA, Brown K, et al. A placebo-controlled trial of pioglitazone in subjects with nonalcoholic steatohepatitis. The New England journal of medicine. 2006; 355:2297–2307. [PubMed: 17135584]
10. Gastaldelli A, Harrison SA, Belfort-Aguilar R, et al. Importance of changes in adipose tissue insulin resistance to histological response during thiazolidinedione treatment of patients with nonalcoholic steatohepatitis. Hepatology. 2009; 50:1087–1093. [PubMed: 19670459]
11. Cusi K, Orsak B, Bril, et al. Long-Term Pioglitazone Treatment for Patients With Nonalcoholic Steatohepatitis and Prediabetes or Type 2 Diabetes Mellitus: A Randomized Trial. Ann Intern Med. 2016; 165:305–315. [PubMed: 27322798]
12. Rizos CV, Kei A, Elisaf MS. The current role of thiazolidinediones in diabetes management. Arch Toxicol. 2016; 90:1861–1881. [PubMed: 27165418]
13. Kersten S. Physiological regulation of lipoprotein lipase. Biochimica et biophysica acta. 2014; 1841:919–933. [PubMed: 24721265]
14. Zhang R. The ANGPTL3-4-8 model, a molecular mechanism for triglyceride trafficking. Open Biol. 2016; 6:150272. [PubMed: 27053679]
15. Petersen KF, Dufour S, Hariri A, et al. Apolipoprotein C3 gene variants in nonalcoholic fatty liver disease. The New England journal of medicine. 2010; 362:1082–1089. [PubMed: 20335584]
16. Pollex RL, Ban MR, Young TK, et al. Association between the −455T>C promoter polymorphism of the APOC3 gene and the metabolic syndrome in a multi-ethnic sample. BMC Med Genet. 2007; 8:80. [PubMed: 18096054]
17. Quagliarini F, Wang Y, Kozlitina J, et al. Atypical angiopoietin-like protein that regulates ANGPTL3. Proceedings of the National Academy of Sciences of the United States of America. 2012; 109:19751–19756. [PubMed: 23150577]

18. Yi P, Park JS, Melton DA. Betatrophin: a hormone that controls pancreatic beta cell proliferation. Cell. 2013; 153:747–758. [PubMed: 23623304]
19. Cox AR, Barrandon O, Cai EP, et al. Resolving Discrepant Findings on ANGPTL8 in beta-Cell Proliferation: A Collaborative Approach to Resolving the Betatrophin Controversy. PloS one. 2016; 11:e0159276. [PubMed: 27410263]
20. Gomez-Ambrosi J, Pascual-Corrales E, Catalan V, et al. Altered Concentrations in Dyslipidemia Evidence a Role for ANGPTL8/Betatrophin in Lipid Metabolism in Humans. The Journal of clinical endocrinology and metabolism. 2016; 101:3803–3811. [PubMed: 27472196]
21. Ren G, Kim JY, Smas CM. Identification of RIFL, a novel adipocyte-enriched insulin target gene with a role in lipid metabolism. American journal of physiology Endocrinology and metabolism. 2012; 303:E334–351. [PubMed: 22569073]
22. Haller JF, Mintah IJ, Shihanian LM, et al. ANGPTL8 requires ANGPTL3 to inhibit lipoprotein lipase and plasma triglyceride clearance. Journal of lipid research. 2017
23. Nidhina Haridas PA, Soronen J, Sadevirta S, et al. Regulation of Angiopoietin-Like Proteins (ANGPTLs) 3 and 8 by Insulin. The Journal of clinical endocrinology and metabolism. 2015; 100:E1299–1307. [PubMed: 26204133]
24. Wang Y, Quagliarini F, Gusarova V, et al. Mice lacking ANGPTL8 (Betatrophin) manifest disrupted triglyceride metabolism without impaired glucose homeostasis. Proceedings of the National Academy of Sciences of the United States of America. 2013; 110:16109–16114. [PubMed: 24043787]
25. Bogan JS, McKee AE, Lodish HF. Insulin-responsive compartments containing GLUT4 in 3T3-L1 and CHO cells: regulation by amino acid concentrations. Molecular and cellular biology. 2001; 21:4785–4806. [PubMed: 11416153]
26. Yu C, Chen Y, Cline GW, et al. Mechanism by which fatty acids inhibit insulin activation of insulin receptor substrate-1 (IRS-1)-associated phosphatidylinositol 3-kinase activity in muscle. The Journal of biological chemistry. 2002; 277:50230–50236. [PubMed: 12006582]
27. Samuel VT, Liu ZX, Wang A, et al. Inhibition of protein kinase Cepsilon prevents hepatic insulin resistance in nonalcoholic fatty liver disease. The Journal of clinical investigation. 2007; 117:739–745. [PubMed: 17318260]
28. Vatner DF, Weismann D, Beddow SA, et al. Thyroid hormone receptor-beta agonists prevent hepatic steatosis in fat-fed rats but impair insulin sensitivity via discrete pathways. American journal of physiology Endocrinology and metabolism. 2013; 305:E89–E100. [PubMed: 23651850]
29. Lee HY, Birkenfeld AL, Jornayvaz FR, et al. Apolipoprotein CIII overexpressing mice are predisposed to diet-induced hepatic steatosis and hepatic insulin resistance. Hepatology. 2011; 54:1650–1660. [PubMed: 21793029]
30. Kumashiro N, Erion DM, Zhang D, et al. Cellular mechanism of insulin resistance in nonalcoholic fatty liver disease. Proceedings of the National Academy of Sciences of the United States of America. 2011; 108:16381–16385. [PubMed: 21930939]
31. Qu X, Seale JP, Donnelly R. Tissue and isoform-selective activation of protein kinase C in insulin-resistant obese Zucker rats - effects of feeding. J Endocrinol. 1999; 162:207–214. [PubMed: 10425458]
32. Pfaffl MW. A new mathematical model for relative quantification in real-time RT-PCR. Nucleic acids research. 2001; 29:e45. [PubMed: 11328886]
33. Sando JJ, Beals JK. Enzyme assays for protein kinase C activity. Methods Mol Biol. 2003; 233:63–76. [PubMed: 12840498]
34. Ping P, Zhang J, Huang S, et al. PKC-dependent activation of p46/p54 JNKs during ischemic preconditioning in conscious rabbits. The American journal of physiology. 1999; 277:H1771–1785. [PubMed: 10564130]
35. Petrick A, Benotti P, Wood GC, et al. Utility of Ultrasound, Transaminases, and Visual Inspection to Assess Nonalcoholic Fatty Liver Disease in Bariatric Surgery Patients. Obes Surg. 2015; 25:2368–2375. [PubMed: 26003548]
36. Gerhard GS, Styer AM, Strodel WE, et al. Gene expression profiling in subcutaneous, visceral and epigastric adipose tissues of patients with extreme obesity. Int J Obes (Lond). 2014; 38:371–378. [PubMed: 23949615]

37. Wood GC, Chu X, Manney C, et al. An electronic health record-enabled obesity database. BMC Med Inform Decis Mak. 2012; 12:45. [PubMed: 22640398]

38. Turpin SM, Nicholls HT, Willmes DM, et al. Obesity-induced CerS6-dependent C16:0 ceramide production promotes weight gain and glucose intolerance. Cell metabolism. 2014; 20:678–686. [PubMed: 25295788]

39. Raichur S, Wang ST, Chan PW, et al. CerS2 haploinsufficiency inhibits beta-oxidation and confers susceptibility to diet-induced steatohepatitis and insulin resistance. Cell metabolism. 2014; 20:687–695. [PubMed: 25295789]

40. Blachnio-Zabielska AU, Chacinska M, Vendelbo MH, Zabielski P. The Crucial Role of C18-Cer in Fat-Induced Skeletal Muscle Insulin Resistance. Cell Physiol Biochem. 2016; 40:1207–1220. [PubMed: 27960149]

41. Petersen MC, Madiraju AK, Gassaway BM, et al. Insulin receptor Thr1160 phosphorylation mediates lipid-induced hepatic insulin resistance. The Journal of clinical investigation. 2016; 126:4361–4371. [PubMed: 27760050]

42. Samuel VT, Shulman GI. The pathogenesis of insulin resistance: integrating signaling pathways and substrate flux. The Journal of clinical investigation. 2016; 126:12–22. [PubMed: 26727229]

43. Liu D, Li S, He H, et al. Increased circulating full-length betatrophin levels in drug-naive metabolic syndrome. Oncotarget. 2017; 8:17510–17517. [PubMed: 28177922]

44. Ebert T, Kralisch S, Hoffmann A, et al. Circulating angiopoietin-like protein 8 is independently associated with fasting plasma glucose and type 2 diabetes mellitus. J Clin Endocrinol Metab. 2014; 99:E2510–2517. [PubMed: 25325797]

45. Fu Z, Berhane F, Fite A, Seyoum B, Abou-Samra AB, Zhang R. Elevated circulating lipasin/betatrophin in human type 2 diabetes and obesity. Sci Rep. 2014; 4:5013. [PubMed: 24852694]

46. von Loeffelholz C, Pfeiffer AF, Lock JF, et al. ANGPTL8 (Betatrophin) is Expressed in Visceral Adipose Tissue and Relates to Human Hepatic Steatosis in Two Independent Clinical Collectives. Horm Metab Res. 2017; 49:343–349. [PubMed: 28351093]

47. Zhang R. Lipasin, a novel nutritionally-regulated liver-enriched factor that regulates serum triglyceride levels. Biochemical and biophysical research communications. 2012; 424:786–792. [PubMed: 22809513]

48. Gusarova V, Banfi S, Alexa-Braun CA, et al. ANGPTL8 Blockade With a Monoclonal Antibody Promotes Triglyceride Clearance, Energy Expenditure and Weight Loss in Mice. Endocrinology. 2017; 158:1252–1259. [PubMed: 28204173]

Research in context

What is already known about this subject?

- Increased lipid deposition at ectopic sites, such as liver and muscle, can cause insulin resistance, while therapies that decrease ectopic lipid improve insulin sensitivity
- Angiopoietin-like 8 (ANGPTL8) is a member of a class of proteins that inhibit lipoprotein lipase, a key regulator of tissue triacylglycerol uptake

What is the key question?

- Can pharmacological knockdown of ANGPTL8 improve white adipose tissue (WAT) lipid uptake, thereby preventing ectopic lipid deposition and insulin resistance?

What are the new findings?

- ANGPTL8 expression is increased in the visceral WAT of obese insulin-resistant individuals compared with equally obese but insulin-sensitive individuals
- Knockdown of ANGPTL8 in fat-fed rodents improves subcutaneous WAT lipoprotein lipase activity and adipose uptake of mealtime triacylglycerol, prevents hepatic steatosis and reverses lipid-induced hepatic insulin resistance

How might this impact clinical practice in the foreseeable future?

- Tissue-specific modulation of lipoprotein lipase activity, potentially through targeting ANGPTL8, is a promising new therapeutic strategy for non-alcoholic fatty liver disease and diet-induced insulin resistance

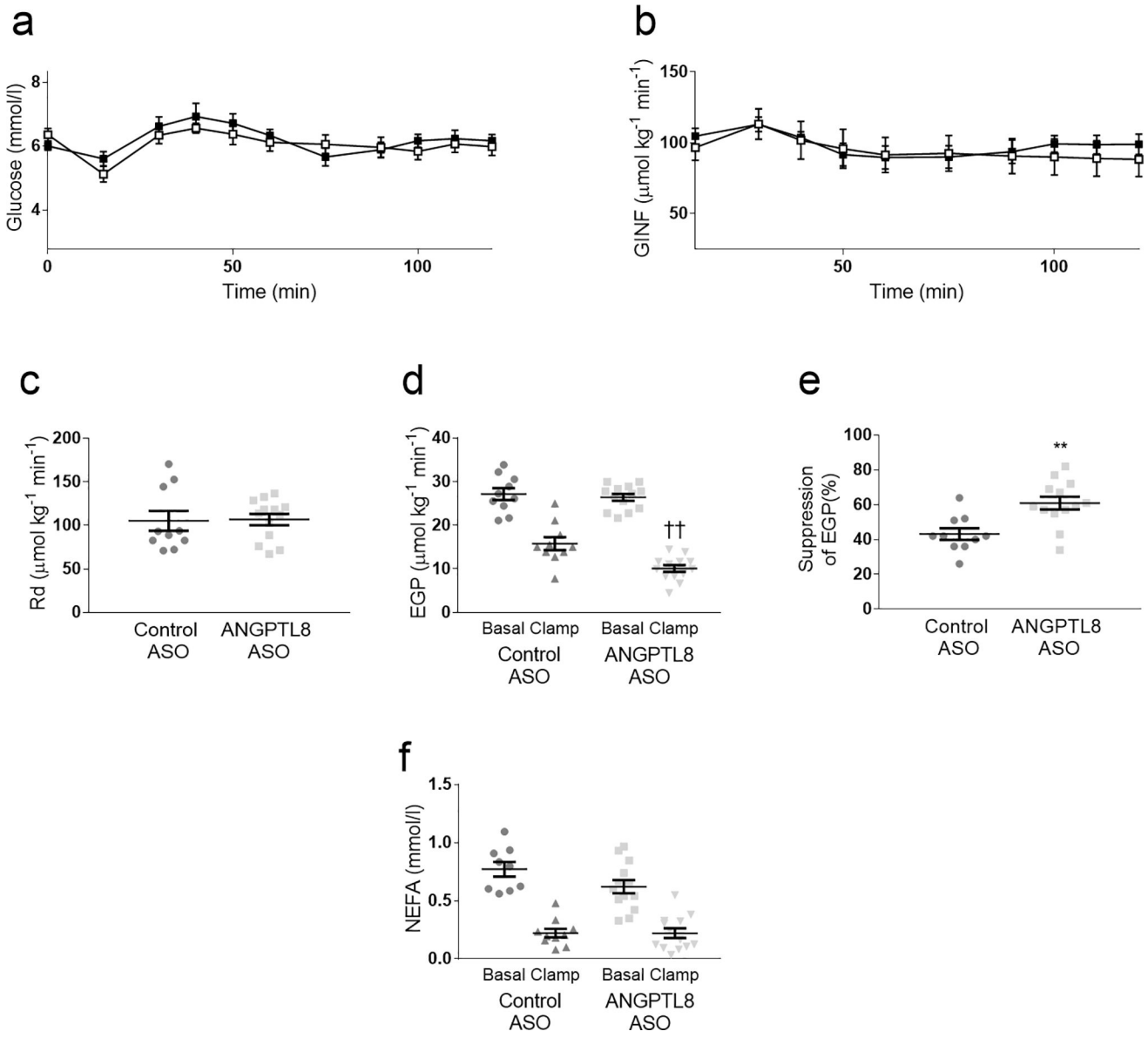

Fig. 1.

Hyperinsulinaemic–euglycaemic clamps. Control ASO- and *Angptl8* ASO-treated rats underwent hyperinsulinaemic–euglycaemic clamps. (**a**) Plasma glucose and (**b**) Glucose infusion rate (GINF) time course throughout the clamp procedure (white squares: control ASO; black squares: *Angptl8* ASO) (**c**) Whole-body insulin-stimulated glucose disposal (Rd). (**d**) Endogenous glucose production (EGP) measured in both the basal and clamped condition. (**e**) Insulin-mediated suppression of endogenous glucose production. (**f**) Plasma NEFA concentrations in basal and clamped conditions. In all figure parts, data are the mean ± SEM of $n = 10$ (control ASO) or $n = 13$ (*Angptl8* ASO). ** $p < 0.01$; $^{\dagger\dagger}p < 0.01$ *Angptl8* ASO clamp vs control clamp

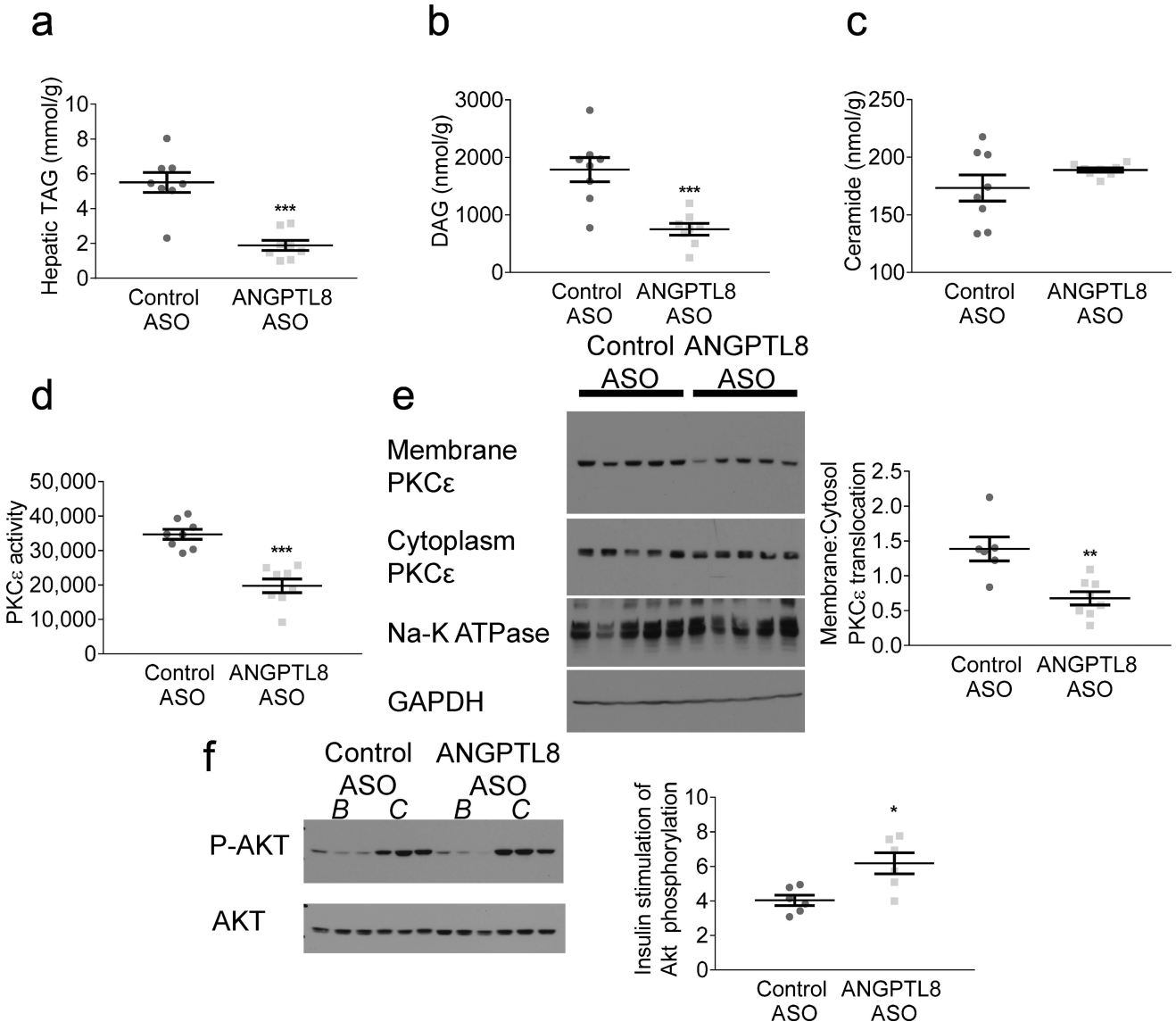

Fig. 2.

Hepatic lipid content and hepatic insulin signalling. (**a**) Hepatic triacylglycerol (TAG) content after a 6 h fast. (**b**) Hepatic DAG content after a 6 h fast. (**c**) Hepatic ceramide content after a 6 h fast. (**d**) Hepatic cell lysate PKCε activity and (**e**) PKCε translocation after a 6 h fast. Membrane:cytoplasm ratio quantified with respect to housekeeping proteins Na-K ATPase and glyceraldehyde-3-phosphate dehydrogenase (GAPDH). Graph in (e) represents membrane:cytoplasm PKCε abundance ratio. (**f**) Hepatic Akt phosphorylation, comparing basal (*B*) 6 h fasted livers with clamped (*C*) insulin-stimulated livers. Graph represents the ratio of Akt phosphorylation in the insulin-stimulated state to Akt phosphorylation in the basal state. For hepatic lipids and PKCε activity, data are the mean ± SEM of $n = 8$; for PKCε translocation, data are the mean ± SEM of $n = 6$ (control ASO) and mean ± SEM of $n = 8$ (*Angptl8* ASO); for hepatic Akt phosphorylation, data are the mean ± SEM of $n = 6$. * $p < 0.05$; ** $p < 0.01$; *** $p < 0.001$ vs control

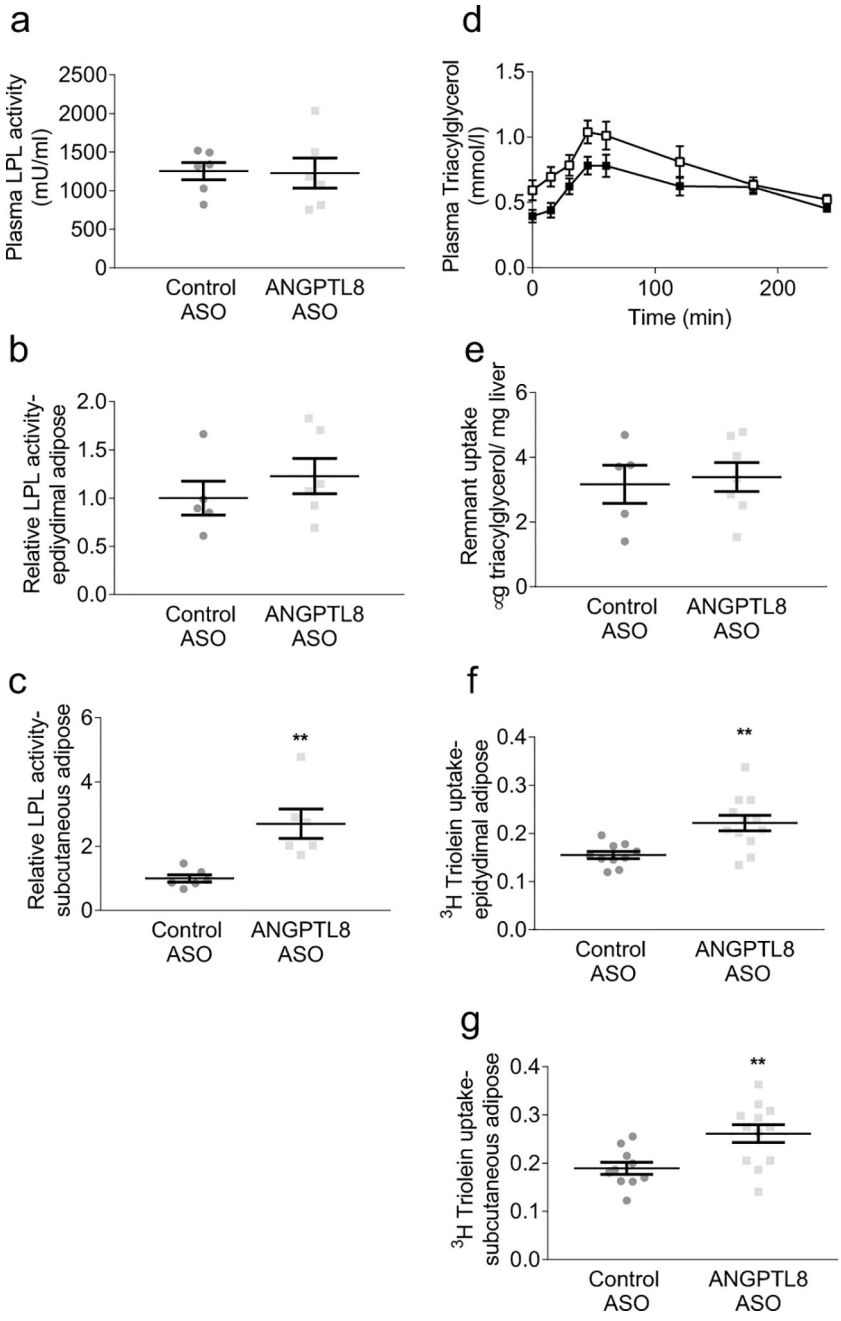

Fig. 3.

LPL activity and tissue triacylglycerol uptake. LPL activity was determined in plasma and tissues of rats euthanised in the fed state. MMTTs were performed in fat-fed rats after an overnight fast. Tissue lipid uptake was assessed 4 h after delivery of mixed meal. (**a**) Plasma LPL activity. (**b**) Epididymal adipose LPL activity, expressed relative to control ASO treatment. (**c**) Subcutaneous adipose LPL activity, expressed relative to control ASO treatment. (**d**) Plasma triacylglycerols during the MMTT (white squares: control ASO; black squares: *Angptl8* ASO). (**e**) Hepatic chylomicron remnant uptake assessed by ^{3}H retinyl palmitate incorporation. (**f**) Epididymal adipose tissue triacylglycerol uptake (counts per mg

tissue) normalised to hepatic triacylglycerol uptake (counts per mg tissue). (**g**) Subcutaneous adipose tissue triacylglycerol uptake normalised to hepatic triacylglycerol uptake. For LPL activity measurements, data are the mean ± SEM of $n = 5–6$. For chylomicron remnant uptake, data are the mean ± SEM of $n = 5$ (control ASO) or mean ± SEM of $n = 7$ (*Angptl8* ASO). For plasma triacylglycerol, data are the mean ± SEM of n=10–14 rats per group; for adipose triacylglycerol uptake, data are the mean ± SEM of $n = 10$ (control ASO) or mean ± SEM of $n = 12$ (*Angptl8* ASO). ** $p < 0.01$ vs control

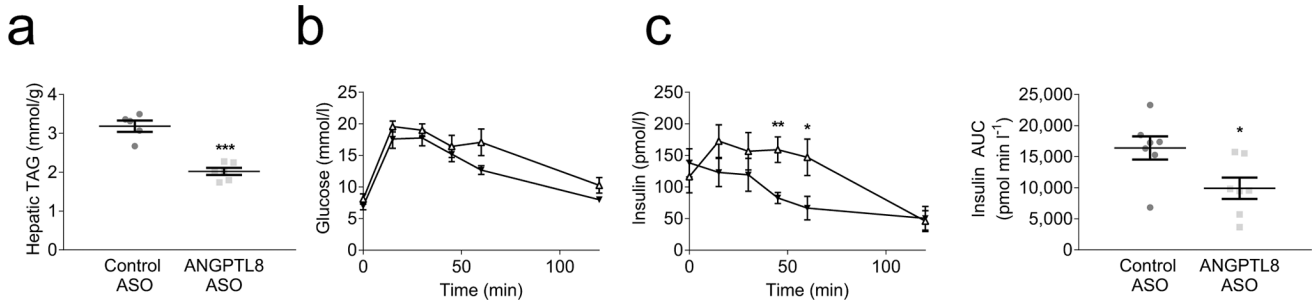

Fig. 4.

Murine protection from hepatic steatosis and glucose intolerance. (**a**) Hepatic triacylglycerol content. (**b, c**) IPGTT (control ASO: white triangles; *Angptl8* ASO: black triangles), measurements of plasma glucose (**b**) and plasma insulin (**c**) presented vs time, together with plasma insulin AUC. For hepatic triacylglycerol, data are the mean ± SEM of $n = 5$ (control ASO) or mean ± SEM of $n = 6$ (*Angptl8* ASO). For IPGTT, data are the mean ± SEM of $n = 8$ (control ASO) or mean ± SEM of $n = 7$ (*Angptl8* ASO). * $p < 0.05$; ** $p < 0.01$; *** $p < 0.001$ vs control

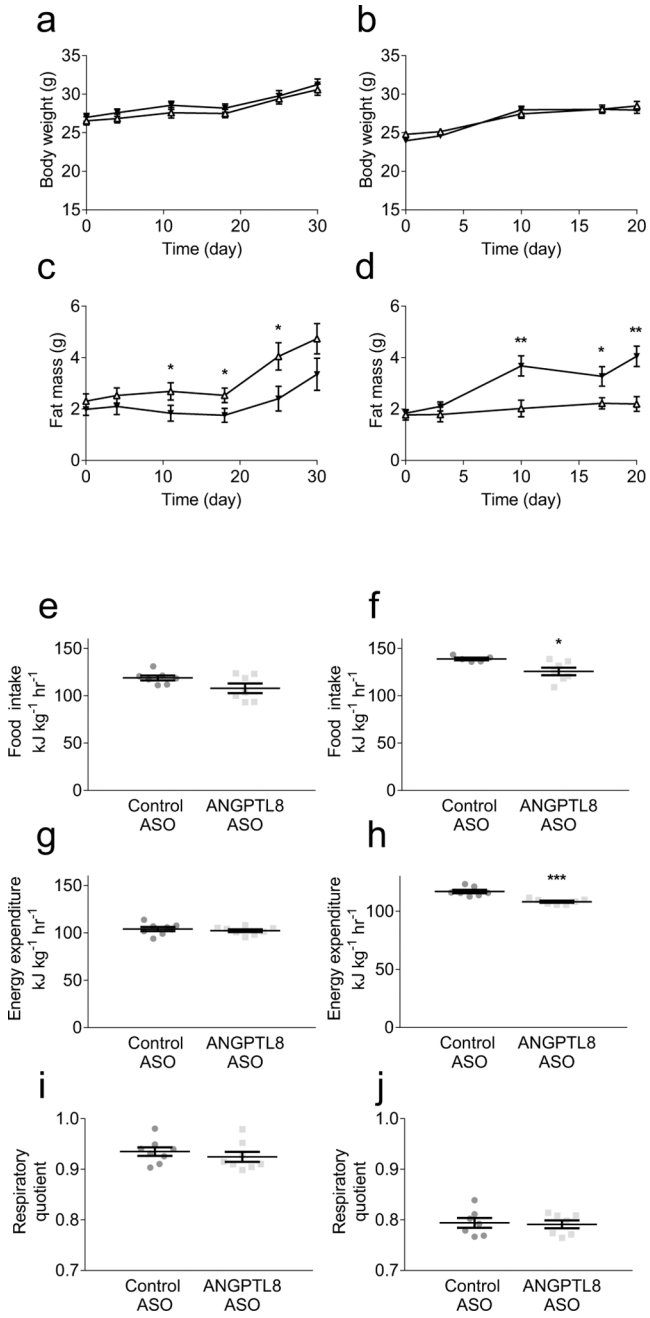

Fig. 5.

Murine growth curves and energy homeostasis. Whole-body adipose content assessed by ^{1}H magnetic resonance spectroscopy; energy homeostasis assessed by metabolic cage analysis: Growth curve in (**a**) RC-fed mice and (**b**) HFD-fed mice. Fat mass accretion in (**c**) RC-fed mice and (**d**) HFD-fed mice (control ASO: white triangles; *Angptl8* ASO: black triangles). Food intake assessed in (**e**) RC-fed mice and (**f**) HFD-fed mice. Energy expenditure assessed in (**g**) RC-fed mice and (**h**) HFD-fed mice. RQ assessed in (**i**) RC-fed mice and (**j**) HFD-fed mice. Metabolic cage variables were normalised to lean body mass. For RC-fed growth curves and fat mass assessments, energy expenditure and RQ data are the mean ± SEM of *n*

= 8 in both groups. For HFD-fed growth curves and fat mass assessments, data are the mean ± SEM of $n = 7$ (control ASO) or mean ± SEM of $n = 8$ (*Angptl8* ASO). For RC-fed food intake, HFD-fed energy expenditure and RQ data are the mean ± SEM of $n = 7$ in both groups. For HFD-fed food intake, data are the mean ± SEM of $n = 5$ (control ASO) or mean ± SEM of $n = 7$ (*Angptl8* ASO). * $p < 0.05$; ** $p < 0.01$; *** $p < 0.001$ vs control

Table 1

Genes and proteins assessed

Genes assessed by qPCR	Proteins assessed by immunoblot
TATA-binding protein (*TBP*)	Akt
Angiopoietin-like 8 (*ANGPTL8*)	Phosphorylated Akt (Ser 473)
β-Actin (*Actb*)	PKCε
Cd68	Sodium–potassium ATPase (Na/K ATPase)
Angiopoietin-like 3 (*Angptl3*)	Glyceraldehyde-3-phosphate dehydrogenase (GAPDH)
Angiopoietin-like 4 (*Angptl4*)	β-Actin
Apolipoprotein C3 (*Apoc3*)	
Apolipoprotein E (*Apoe*)	
Apolipoprotein C1 (*Apoc1*)	
Apolipoprotein A5 (*Apoa5*)	
Hepatic lipase (*Lipc*)	

Immunoblot antibodies and primer sequences for quantitative PCR are available in ESM Table 1 and ESM Table 2

Table 2

Clinical data from patients undergoing bariatric surgery

	Insulin sensitive	Insulin resistant	*p*
BMI (kg/m^2)	50 ± 2	48 ± 3	0.6
HOMA-IR	2.1 ± 0.1	13.5 ± 2.0	< 0.001
Age (years)	40 ± 2	53 ± 3	< 0.01
Cholesterol (mmol/l)	4.61 ± 0.18	4.20 ± 0.39	0.4
LDL-C (mmol/l)	2.82 ± 0.18	2.36 ± 0.34	0.3
HDL-C (mmol/l)	1.24 ± 0.08	0.93 ± 0.05	< 0.01
Plasma triacylglycerols (mmol/l)	1.20 ± 0.19	1.99 ± 0.24	< 0.05
AST (μkat/l)	0.40 ± 0.03	0.80 ± 0.22	0.1
ALT (μkat/l)	0.40 ± 0.05	0.92 ± 0.35	0.2
Liver histology			
NAS score	1.6 ± 0.5	3.5 ± 0.4	< 0.05
Steatosis score	1.0 ± 0.2	1.9 ± 0.2	< 0.01
Inflammation score	0.3 ± 0.2	0.8 ± 0.2	0.09
Ballooning score	0.2 ± 0.1	0.8 ± 0.2	< 0.05
Fibrosis score			
Grade 0	6/9	1/10	
Grade 1a	3/9	5/10	
Grade 1b	0/9	1/10	
Grade 1c	0/9	1/10	
Grade 3–4	0/9	2/10	
Adipose *Angptl8* expression (relative expression)	1.0 ± 0.3	7.6 ± 2.6	< 0.05

AST, aspartate aminotransferase; ALT, alanine aminotransferase; NAS, NAFLD activity score.

Table 3

Variables after 6 h fasting in HFD-fed rats

	Control ASO	***Angptl8* ASO**	***p***
Body weight (g)	457 ± 6	432 ± 15	0.15
Epididymal WAT weight (g)	6.8 ± 0.6	5.5 ± 0.4	0.10
Insulin (pmol/l)	243± 28	111 ± 21	< 0.01
Plasma triacylglycerol (mmol/l)	1.45 ± 0.17	0.59 ± 0.06	< 0.001
NEFA (mmol/l)	0.14 ± 0.01	0.17 ± 0.02	0.12
Glucose (mmol/l)	9.05 ± 0.22	8.49 ± 0.22	0.15
BUN (mmol/l)	3.96 ± 0.21	3.86 ± 0.14	0.76
ALT (μkat/l)	0.52 ± 0.03	0.58 ± 0.07	0.29
AST (μkat/l)	0.87 ± 0.03	1.0 ± 0.1	0.22